We are IntechOpen, the world's leading publisher of Open Access books Built by scientists, for scientists

4,800
Open access books available

122,000
International authors and editors

135M
Downloads

Our authors are among the

154
Countries delivered to

TOP 1%
most cited scientists

12.2%
Contributors from top 500 universities

CLARIVATE ANALYTICS BOOK CITATION INDEX INDEXED

WEB OF SCIENCE™

Selection of our books indexed in the Book Citation Index in Web of Science™ Core Collection (BKCI)

Interested in publishing with us?
Contact book.department@intechopen.com

Numbers displayed above are based on latest data collected.
For more information visit www.intechopen.com

13

Identification of Aquatic Birnavirus VP3 Death Domain and Its Dynamic Interaction Profiles in Early and Middle Replication Stages in Fish Cells

Jiann-Ruey Hong[1,*] and Jen-Leih Wu[2]
[1]*Laboratory of Molecular Virology and Biotechnology, Institute of Biotechnology, National Cheng Kung University*
[2]*Laboratory of Marine Molecular Biology and Biotechnology, Institute of Cellular and Organismic Biology, Academia Sinica, Nankang Taiwan*

1. Introduction

Infectious pancreatic necrosis virus (IPNV) is a fish pathogen and the prototype of the *Birnaviridae* virus family (Dobos et al., 1979). IPNV causes infectious pancreatic necrosis, an acute and serious disease in juvenile salmonid fish worldwide (Hill and Way, 1995) Birnaviruses possess a bi-segmented, double-stranded RNA genome contained within a medium-sized, unenveloped, icosahedral capsid. The protein products of four unrelated major genes undergo various post-translational cleavage processes to generate three to five different structural proteins (Dobos, 1995). The largest of these proteins (VP1; 90–110 kDa) is encoded by the smaller segment B RNA (Wu et al., 1998). The larger genome segment A contains a large open reading frame (ORF; which encodes VP3 [32-kDa; a minor capsid protein] [Wu et al., 1998], VP4 [28 kDa], and VP2 [the major capsid protein; 46 kDa] [Wu et al., 1998]) and a small ORF, which encodes VP5 (17 kDa; a non-structural protein with anti-apoptotic activity) (Hong et al., 2002a; Hong and Wu, 2002c).

Previously, it was found that IPNV-induced apoptosis (Hong et al., 1998; Hong, et al., 1999a; Hong et al., 1999b; Hong and Wu, 2002) may be mediated through activation of caspase-8 and -3 (Hong et al., 2005) and requires new protein synthesis (Hong et al., 1999). This pathway may be triggered through NF-κB transcription factor transactivation of downstream effector genes such as Bad (Hong et al., 2008). Recently, it was found that IPNV-induced loss of $\Delta\Psi m$ can be blocked by the adenine nucleotide translocase (ANT) inhibitor bongkrekic acid (BKA) (Chen et al., 2009), and that IPNV-induced expression of annexin 1 can have an anti-death function (Hwang et al., 2007). IPNV was also found to induce apoptotic cell death and necrotic cell death in the same cells through TNFα up-regulation (Wang et al., 2011).

The structures associated with IPNV replication and genome and particle assembly in infected cells have only started to be elucidated. Recently, viral particles of different sizes

*Corresponding Author

were identified during the IPNV infective cycle (Villanueva et al., 2004). Immediately after synthesis, non-infectious, immature particles 66 nm in diameter appeared. These provirion particles were detected simultaneously with viral double-stranded (ds) RNA in infected cells, suggesting that viral assembly occurs as soon as dsRNA replication has begun. Subsequent maturation into smaller virions (60 nm in diameter) was found to proceed through proteolytic cleavage of the viral precursors within the capsid. An early study of IPNV also suggested an association of VP3 with viral RNA. VP3-containing ribonucleoprotein core structures were identified by electron microscopy studies, and an association of the basic C-terminal end of the protein with the viral genome was proposed (Hudson et al., 1986). Furthermore, Pedersen found that VP3 can interact with itself, co-precipitate dsRNA, and interact with VP1 (Pedersen et al., 2007). The dynamics of VP3 interaction with other proteins or RNA are still unknown.

In the present study, we located the death domain of VP3 protein and examined its interactions with other viral molecules culminating in the formation of the VP3-VP1-RNA-VP2 complex during viral replication.

2. Materials and methods

2.1 Cell line and virus

Chinook salmon embryo cells (CHSE-214 obtained from the American Type Culture Collection, ATCC, Manassas, VA, USA) were grown at 18°C in plastic tissue-culture flasks (Nalge Nunc International, Rochester, NY, USA) containing Eagle's minimum essential medium (MEM) supplemented with 10% (v/v) fetal bovine serum (FBS) and gentamycin (25 µg/ml). ZLE cells were grown at 28°C in Leibovitz's L-15 medium (GibcoBRL, Grand Island, NY) supplemented with 5% v/v FBS and 25 µg/ml of gentamycin. An isolate of the Ab strain of IPNV, designated E1-S, was obtained from Japanese eels in Taiwan (Wu et al., 1987). The virus was propagated in CHSE-214 cell monolayers at a multiplicity of infection (MOI) of 0.01 per cell. Infected cultures were monitored as described previously (Dobos, 1977) and Tissue Culture Infectious Dose 50 ($TCID_{50}$) assay was performed on confluent monolayers (Nicholson and Dunn, 1974).

2.2 VP3-enhanced green fluorescent protein (EGFP) gene fusion and different mutant form constructions

A VP3 coding sequence from IPNV E1S VP3 (VP3 cDNA in pGEMT-easy plasmid) was amplified using the sense primer (1-P1; in Table 1) 5′-CCgCTCgAgCC**ATg**gACgAggAgCTg CAA-3′ (the *Xho* I site is underlined and the start codon of VP3 is in boldface) and an anti-sense primer (1-P2) 5′-CgggATCCATTCACCTCCgCATCTT-3′ (the *Bam*HI site is underlined). This allowed for the construction of VP3-EGFP fusion genes to monitor VP3-induced cellular morphological changes. The other VP3 mutant forms (pEGFP-VP3: 1–158, pEGFP-VP3: 80–237, pEGFP-VP3: 80–158, pEGFP-VP3: 1–79, and pEGFP-VP3: 159–237) were amplified using the sense primers (2-P1, 2-P1, 4-P1, 5-P1, and 6-P1; in Table 1) and an anti-sense primer (2-P2, 3-P2, 4-P2, 5-P2, or 6-P2; in Table 1). The *Xho* I and *Bam*HI sites are underlined in the constructions shown in Table 1. PCR products were ligated with the identically predigested pEGFP (enhanced yellow fluorescent protein)-C1 vector (BD Biosciences ClonTech, Palo Alto, CA, USA) after restriction digestion with *Xho* I and *Bam*HI to create pEGFP-VP3. Cell transfection was implemented by seeding 3 x 10^5 ZLE cells in 60-

mm culture dishes one day prior to the transfection procedure. pEGFP, pEGFP-VP3, and each of the VP3 deletion mutant forms (2 μg) were separately transfected into cells using Lipofectamine-Plus (Life Technologies, Inc., Gaithersburg, MD). Expression of the EYFP fusion proteins was visualized using a fluorescence microscope with an FITC filter set, as previously described (Hong et al., 1999b). The number of apoptotic cells containing EGFP or EGFP-VP3 (200 cells per sample) was assessed for three individual experiments. Each point represents the mean number of apoptotic cells ± the standard error of the mean (SEM). Data were analyzed using either the paired or unpaired Student's *t*-test as appropriate. Statistical significance of between-group differences in mean values was defined at $P < 0.05$.

2.3 Western blot analysis

CHSE-214 cells (4.0 ml) were seeded at 10^5 cells per ml per 60 mm Petri dish for at least 20 h prior to cultivation. The resulting monolayers were rinsed twice with PBS. Cells were infected with virus at an MOI of 1.0 and were incubated for 0, 4, 6, 8, 12, or 24 h. Culture media were aspirated at the end of each time point. Cells were washed with PBS and lysed in 0.3 ml of lysis buffer (10 mM Tris base, 20% glycerol, 10 mM sodium dodecyl sulfate, and 2% β-mercaptoethanol; pH = 6.8). ZLE cells (4.0 ml) were seeded at $1x10^5$ cells per ml and cultivated as previously described for VP3 to allow mutant gene overexpression. The cells after 20 h were transfected with pEGFP, pVP3-EGFP, pEGFP-VP3: 1–158, pEGFP-VP3: 80–237, pEGFP-VP3: 80–158, pEGFP-VP3: 1–79, and pEGFP-VP3: 159–237 plasmids (2 μg added to each dish) using Lipofectamine-Plus (Life Technologies). Transfection was allowed to proceed for 4 h. ZLE cells were incubated at 28°C for 0, 24, and 48 h. Culture media were aspirated at the end of each incubation period. The cells were washed with PBS and finally lysed in 0.3 ml of lysis buffer.

Proteins were separated by sodium dodecyl sulfate-polyacrylamide gel electrophoresis (Laemmli, 1970), electroblotted, and visualized using a previously described method (Kain et al., 1994). Blots were incubated first with anti-IPNV E1-S polyclonal antibodies (PolyAb, 1:1500) (Hong et al., 1999a), anti-mouse β-actin MAb (1:5000; Chemicon, Temecula, CA, USA), or anti-mouse EGFP MAb (1:3000, Clontech Laboratories, Mountain View, CA, USA), then with peroxidase-labeled goat anti-mouse conjugate (1:7500 to 1:10,000; Amersham, Piscataway, NJ, USA) or peroxidase-labeled goat anti-rabbit conjugate (1:7500 to 1:10,000; Amersham).

Chemiluminescence detection was performed using the Western Exposure Chemiluminescence Kit (Amersham) according to the manufacturer's instructions. Chemiluminescence was visualized on Kodak XAR-5 film (Eastman Kodak, Rochester, NY, USA), and protein expression level amounts were quantified using a Personal Densitometer (Molecular Dynamic, Sunnyvale, CA).

2.4 Radioactive labeling of infected cells for determination of VP3 interactions

Radioactive labeling of infected cells: A confluent CHSE-214 cell monolayer in a plastic tissue culture plate (60 mm diameter, Nunc) was infected with IPN virus at 18°C at an MOI of 1. After a 1-h adsorption period, the medium was removed, the monolayer was rinsed three times with phosphate-buffered saline (PBS), and starved for 2 h at 18°C. Then, growth medium containing 50 μCi ml^{-1} of [^{35}S]methionine was added. At different times in the

labelling period (3–20 h) or continuously labelled for 20 h as a positive control, the cell layer was washed with PBS, and the monolayer was lysed in 1 ml of lysis buffer (0.5% [v/v] Nonidet P-40 in phosphate-buffered saline) (Wu et al., 1998).

VP3 interaction assay: Cell extracts were incubated for 18 h at 4°C in the presence of 0.1% (w/v) *N*-laurolysarcosine, 1% bovine serum albumin, 10 M phenylmethanesulfonyl fluoride (PMSF), and anti-mouse E1S VP3 B9 and E7 monoclonal antibodies (home-made). The mixture was incubated with anti-rabbit IgG serving as a negative control) 1 µg/ ml each antibody; Transduction Laboratories, Lexington, KY) at 4°C for 12 h, and then with 160 µl of 10% (v/v) protein A-Sepharose (Zyme) in 150 mM NaCl/10 mM Tris-HCl, pH 7.8/1% *N*-lauroylsarcosine at 4°C for 1 h. The protein A-Sepharose-antibody complexes so formed were washed three times in the same buffer, boiled in 200 µl of 10 mM Tris-HCl, pH 7.8/1 mM EDTA/0.1% SDS (Hong and Wu. 2002), and boiled in 60 µl of sodium dodecyl sulfate (SDS)-polyacrylamide gel electrophoresis (PAGE) sample buffer containing 5% SDS and 4% β-mercaptoethanol to release bound proteins. Proteins present in the cell lysate were separated by SDS-polyacrylamide gel electrophoresis (Laemmli, 1970), and the dried gel (dried under vacuum) (Studier, 1973) was autoradiographed.

3. Results

3.1 VP3 expressed early in the replication cycle

The present study confirmed that a minor viral capsid protein VP3 is expressed early in the IPNV replication cycle (Wu et al., 1987; Wu et al., 1998). VP3 expression levels increased 5-fold between 4 and 6 h post-infection (p.i.) (Fig. 1A, lanes 2 and 3) compared to levels in mock-infected normal control cells (Fig. 1A, lane 1). The elevated expression was maintained for 8–24 h p.i. (Fig. 1A, lanes 4–7).

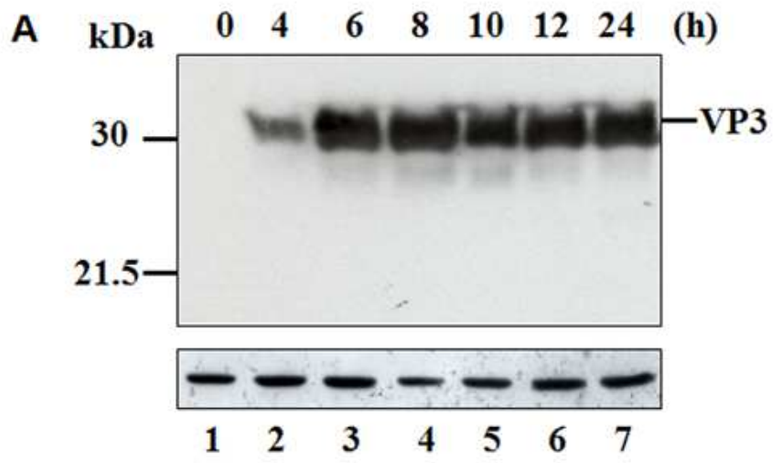

Fig. 1. IPNV VP3 protein expression in CHSE-214 cells.
The pattern of VP3 expression in CHSE-214 cells was revealed using a anti-IPNV E1-S particle polyclonal antibody. The cells were infected with IPNV (MOI=1), lysed at different times p.i., and the proteins in lysates were separated electrophoretically. Lane 1 corresponds to IPNV-uninfected cells (0 h; the control). Lanes 2–7 correspond to IPNV-infected cells lysed 4, 6, 8, 10, 12, and 24 h p.i., respectively.

3.2 VP3 localization

Green fluorescent protein (GFP) from the jellyfish *Aequorea victoria* has become an invaluable tool for monitoring gene expression and fusion protein localization *in vivo* or *in situ*, as well as for determination of cellular morphological changes (Chalfie et al., 1994; Hong et al., 1999b; Maniak et al., 1995; Oparka et al., 1997). A variant type of GFP (EGFP), a marker for visualization of apoptotic cell morphological changes (Hong et al., 1999b), was used in the present study to trace VP3 localization and monitor interaction with other proteins.

The tracking of VP3 with EGFP in ZLE cells has revealed their presence in plasma (Espinoza et al., 2000). However, VP3 was absent from endoplasmic reticulum (ER) when tracked with an ER marker (data not shown).

3.3 Identification of the VP3 death-inducing domain

Recently, we demonstrated that IPNV VP3 induces apoptotic cell death through the up-regulation of the pro-apoptotic effector Bad, which triggers the mitochondria-mediated cell death pathway (Chiu et al., 2010). A deletion series was used to determine which VP3 region might be associated with death induction. Different VP3 constructs were designed (Fig. 2A; Table 1) and inserted into pEGFP to produce pEGFP-VP3 (VP3 full length, 1–237 aa), pEGFP-VP3: 1–158, pEGFP-VP3: 80–237, pEGFP-VP3: 80–158, pEGFP-VP3: 1–79, and pEGFP-VP3: 159–237. All were amplified for further identification. Western blotting with anti-EGFP monoclonal antibody confirmed the different sizes of EGFP (lane 1), EGFP-VP3 (lane 2), EGFP-VP3: 1–158 (lane 3), EGFP-VP3: 80–237 (lane 4), EGFP-VP3: 80–158 (lane 5), EGFP-VP3: 1–79 (lane 6), and EGFP-VP3: 159–237 (lane 7) transiently expressed 48 h p.i. (Fig. 2B).

Construction of vectors	Primer sequences
pEGFP-VP3	1-P1: 5'-CCG**CTCGAG**CCATGGACGAGGAGCTGCAA-3' 1-P2: 5'-CG**GGATCC**ATTCACCTCCGCATCTT-3'
pEGFP-VP3:1-158	2-P1: 5'-CCGCTCGAGCCATGGACGAGGAGCTGCAA-3' 2-P2: 5'-CG**GGATCC**GCCGTACACACTGTTGG-3'
pEGFP-VP3:80-237	3-P1: 5'-CCG**CTCGAG**CCGAGGCGAGAGCCGTTCGCATCT-3' 3-P2: 5'-CGG**GATCC**ATTCACCTCCGCATCTT-3'
pEGFP-VP3:80-158	4-P1: 5'-CCG**CTCGAG**CCGAGGCGAGAGCCGTTCGCATCT-3' 4-P2: 5'-CG**GGATCC**GCCGTACACACTGTTGG-3'
pEGFP-VP3:1-79	5-P1: 5'-CCG**CTCGAG**CCATGGACGAGGAGCTGCAA-3' 5-P2: 5'-CG**GGATCCT**TGGGCGGCATGCTGGTT-3'
pEGFP-VP3:159-237	6-P1: 5'-CCGC**TCGAG**CCCTCCCGCACCAGGAACCAGCC-3' 6-P2: 5'-CG**GGATCC**ATTCACCTCCGCATCTT-3'

Notes: P1, designed as for forward primer and P2 as for reverse primer.

Table 1. The primers were used to VP3 and different mutant constructions of EGFP-VP3 fusion genes in plasmids.

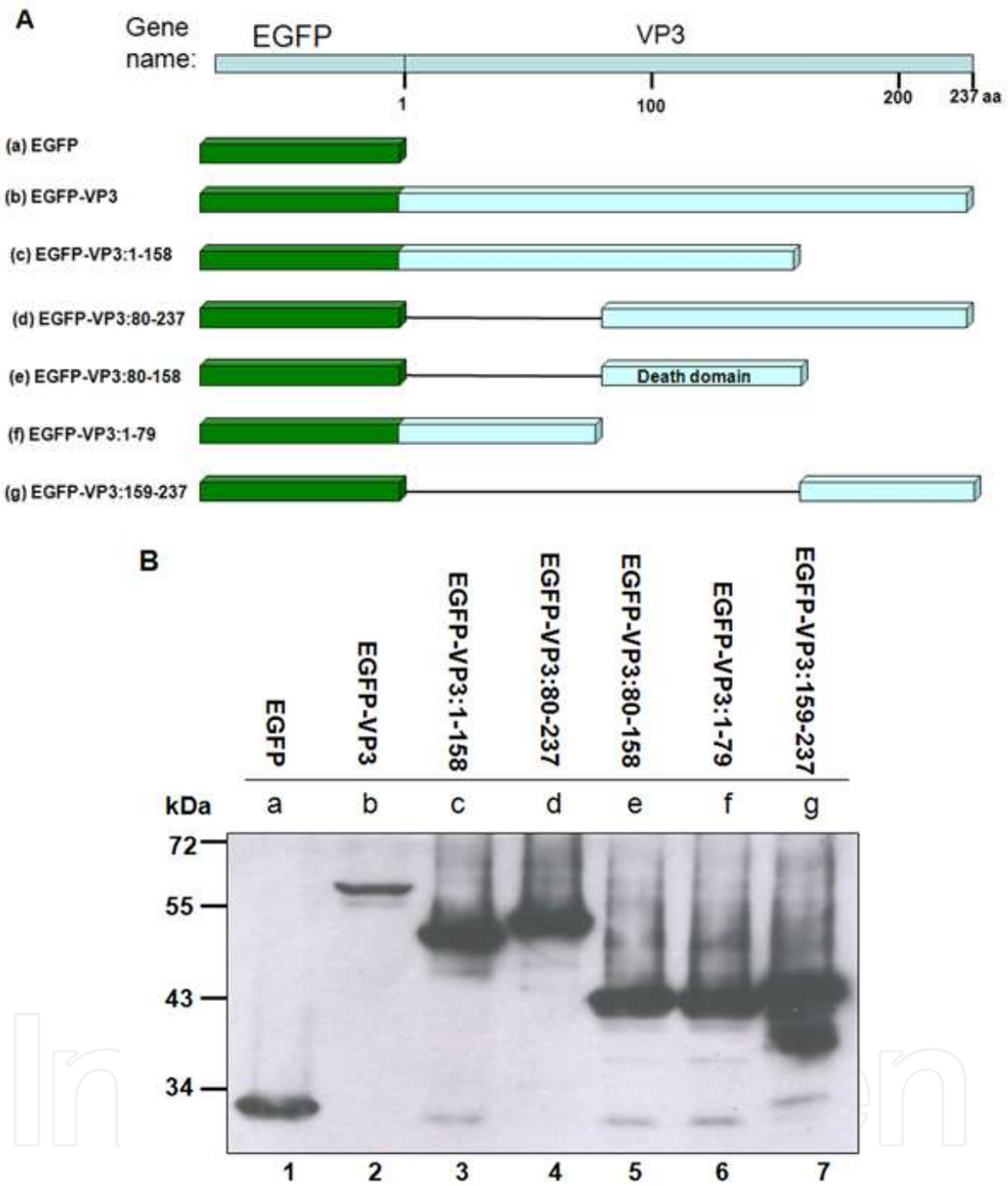

Fig. 2. Mapping and identification of the IPNV VP3 death-inducing domain (80–158 aa) in fish cells. (A) Schematic representation of various IPNV VP3 deletion mutant constructs N-terminally fused with EGFP and transfected into ZLE cells. (B) Identification of EGFP, EGFP-VP3, and EGFP-VP3 deletion mutants. The pEGFP, pEGFP-VP3, and different pEGFP-VP3 mutants were transfected into ZLE cells with Lipofectamine-Plus. The cells were incubated for 48 h post-transfection (lane 1, EGFP; lane 2, EGFP-VP3; lane 3, EGFP-VP3: 1–158; lane 4, EGFP-VP3: 80–237; lane 5, EGFP-VP3: 80–158; lane 6, EGFP-VP3: 1–79, and lane 7, EGFP-VP3: 159–237) and lysed. The lysates were analyzed by Western blotting using a monoclonal antibody to EGFP.

EGFP served as a tracer to allow direct visualization of apoptotic changes in ZLE cells overexpressing VP3 and VP3 peptides at 48 h p.t. The site of the death domain was found to be in a 78-aa region between aa 80 and aa 157 (Fig. 3A). Compared to EGFP-VP3 fusion proteins without this region, those containing this domain induced a higher rate of apoptosis (Fig. 3B; see phase-contrast micrographs in panels b [EGFP-VP3], c [EGFP-VP3: 1–158], d [EGFP-VP3: 80–237], and i [EGFP-VP3: 80–158] and green fluorescence micrographs in panels f [EGFP-VP3], g [EGFP-VP3: 1–158], h [EGFP-VP3: 80–237], and l [EGFP-VP3: 80–158; arrows indicate EGFP-positive cells]). By contrast, the rate of apoptosis was much less in cells expressing EGFP, EGFP-VP3: 1–79, and EGFP-VP3: 159–237 (panels c [EGFP], m [EGFP-VP3: 1–79], and f [EGFP-VP3: 159–237]).

As shown in Figure 3B, these rates at 48 h p.i. were higher in the presence of the death domain (69% [EGFP-VP3], 36% [EGFP-VP3: 1–158], 49% [EGFP-VP3: 80–237], and 52% [EGFP-VP3: 80–158]) than in its absence (3% [EGFP], 18% [EGFP-VP3: 1–79], and 12% [EGFP-VP3: 159–237]).

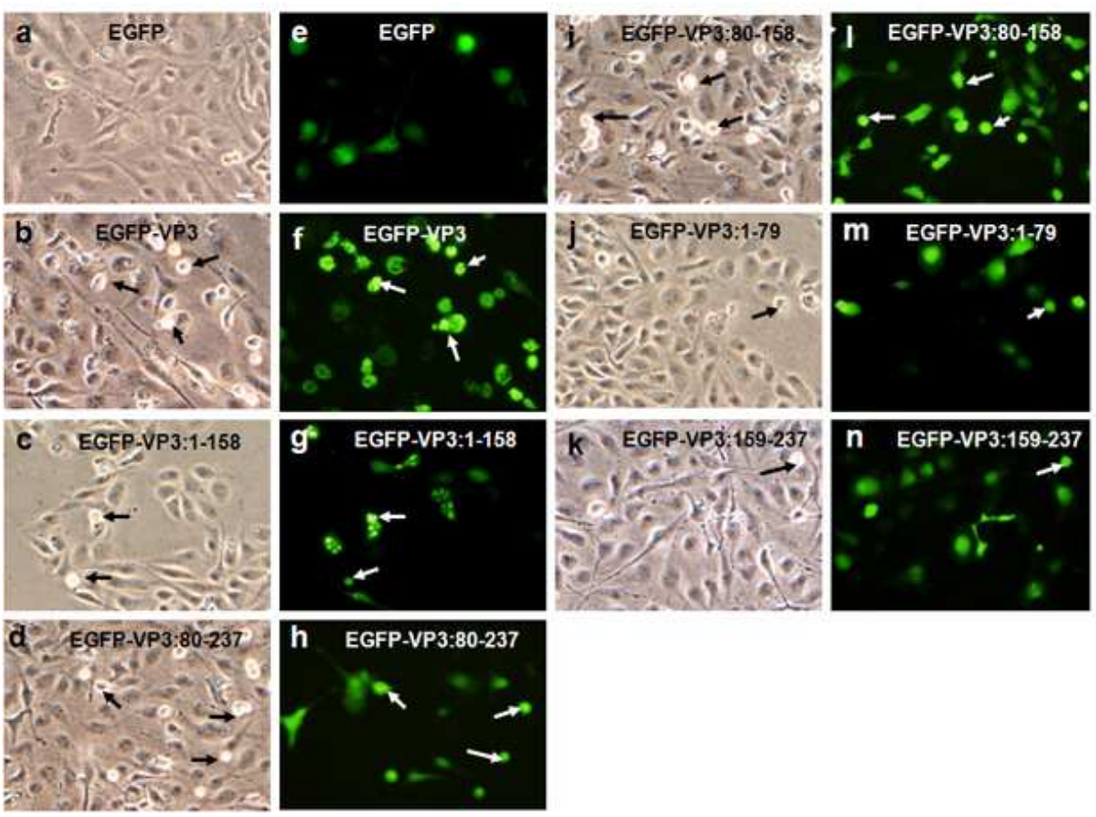

A

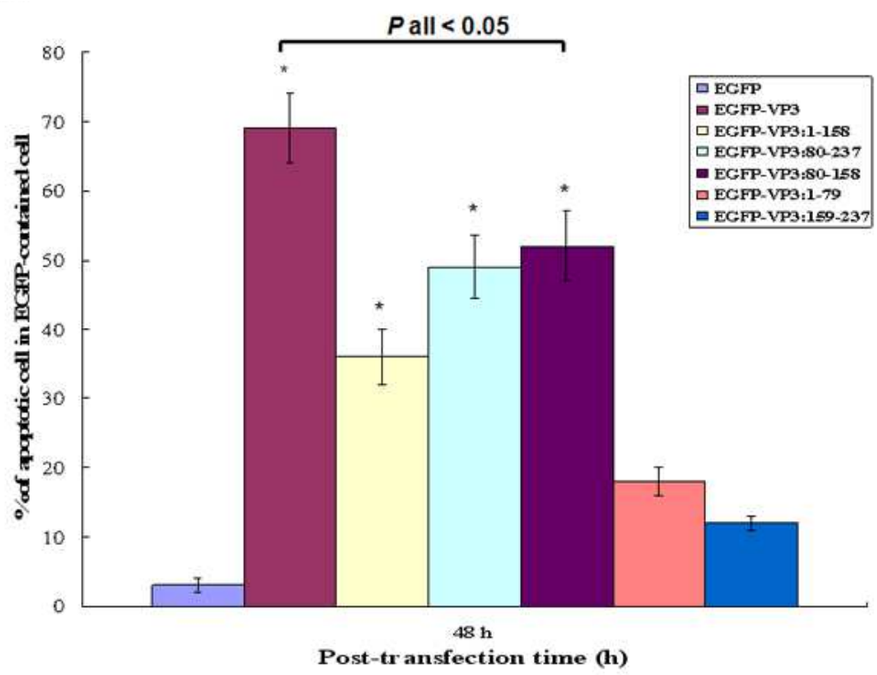

B

Fig. 3. Identification of the death domain of VP3 in ZLE cells.
Expression of EGFP, EGFP-VP3, and EGFP-VP3 deletion mutants was assessed in ZLE cells. The pEGFP, pEGFP-VP3, and different pEGFP-VP3 mutants were transfected into ZLE cells with Lipofectamine-Plus, and the cells were incubated for 48 h post-transfection (p.t.). (A) Phase-contrast and fluorescence micrographs of transfected and untransfected apoptotic ZLE cells at 48 h p.t. Rounded up cells and plasma membrane blebbing are indicated by arrows (Bar = 10 μm). (B) The percentage of apoptotic cells containing EGFP, EGFP-VP3, or the different EGFP-VP3 deletion mutant constructs at 48 h p.t. The number of apoptotic cells per 200 cells per sample was assessed. Each point represents the mean of three independent experiments and the vertical bars indicate ± the standard error of the mean (SEM). Data were analyzed using either paired or unpaired Student's *t*-test as appropriate. Statistical significance was defined at $P < 0.05$.

3.4 Kinetics of VP3 interaction during IPNV infection

Although VP3 participated in many viral processes (apoptosis induction, binding to viral RNA, binding to RdRp, and self interaction), it did not associate directly with capsid protein VP2. So, we were interested in the mechanism of interaction between VP3 protein and other proteins. The binding of native VP3 to two VP3 monoclonal antibodies was assessed at 0, 2.5, 4, 6, 8, and 24 h p.i. (Fig. 4). VP3 protein was found to bind to both anti-VP3 B9 (lanes, 15–20) and anti-VP3 E7 (lanes, 21–26) Mabs at 6, 8, and 24 h p.i. but not to the negative controls protein A (lanes, 3–8) and secondary anti-rabbit Ig (lanes, 9–14). The positive control ([^{35}S]methionine continuously labelled for 20 h) is shown in lane 2 and protein markers labelled with [^{35}S]methionine are shown in lane 1. Furthermore, we found just only anti-VP3 E7 that at 6 h p.i., VP3 associated with VP1, p85 protein, and RNA to form a complex capable of binding VP2 protein during the period 8–24 h p.i (Fig. 5), indicating that viral particle assembly begins as early as 6 h p.i.

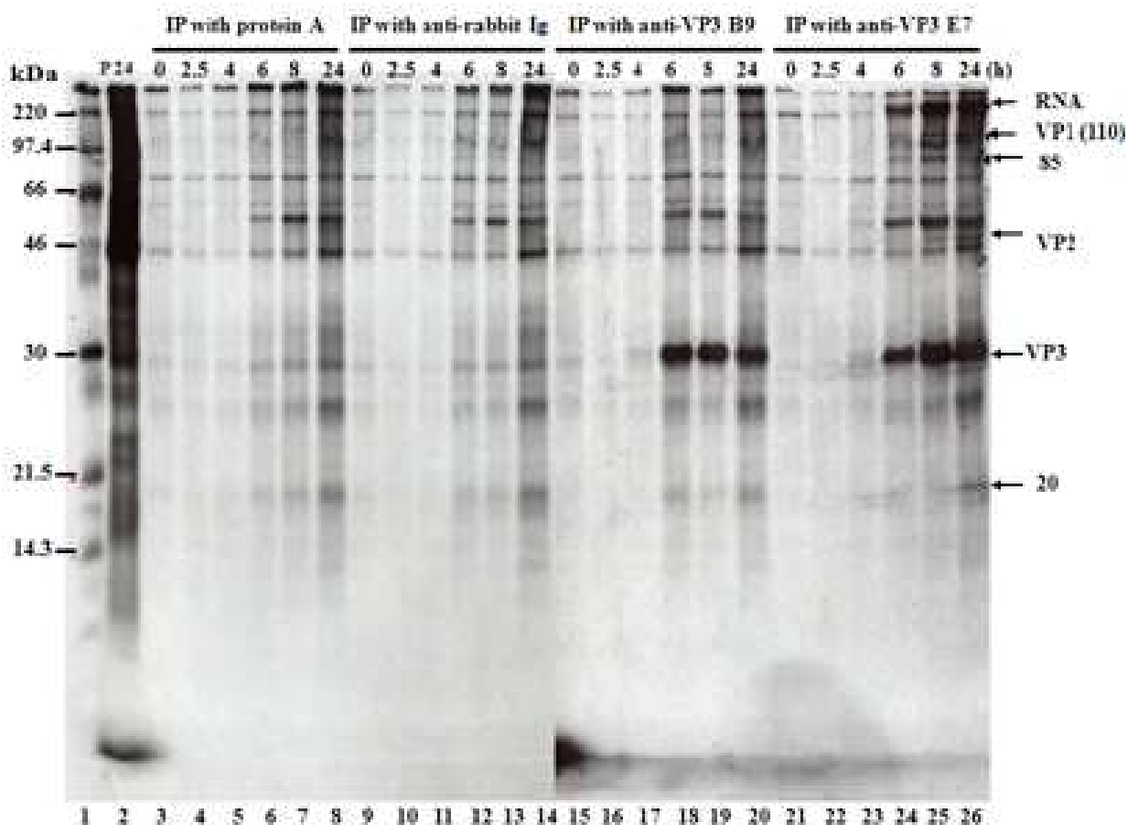

Fig. 4. Identification of profiles of IPNV-VP3 protein interaction with anti-VP3 monoclonal antibody at different replication stages in CHSE-214 cells.
The non-infected and IPNV-infected cells were labelled with [^{35}S]methionine at different times after infection and lysed. The lysates were immunoprecipitated with protein A Sepharose (Zyme) coupled with anti-rabbit Ig, and anti-IPNV-VP3 B9 and anti-IPNV-VP3 E7 monoclonal antibodies, and analyzed on 12% SDS-PAGE. Lane 1, [^{35}S]methionine protein markers; lane 2, lysate of IPNV-infected CHSE-214 cells labelled with [^{35}S]methionine for 20 h; lanes 3–8, [^{35}S]methionine-labelled CHSE-214 cells lysed and reacted with protein A Sepharose (Zyme) at 0, 2.5, 4, 6, 8, and 24 h p.i., respectively; lanes 9–14, [^{35}S]methionine-labelled CHSE-214 cells lysed and reacted with protein A Sepharose (Zyme) coupled to anti-rabbit Ig (Zyme) at 0, 2.5, 4, 6, 8, and 24 h p.i., respectively; lanes 15–20, [^{35}S]methionine-labelled CHSE-214 cells lysed and reacted with protein A Sepharose (Zyme) coupled to anti-IPNV-VP3 B9 (home-made) at 0, 2.5, 4, 6, 8 and 24 h p.i., respectively; lanes 21–26, [^{35}S]methionine-labelled CHSE-214 cells lysed and reacted with protein A Sepharose (Zyme) coupled to anti-IPNV-VP3 E7 (home-made) at 0, 2.5, 4, 6, 8 and 24 h p.i., respectively.

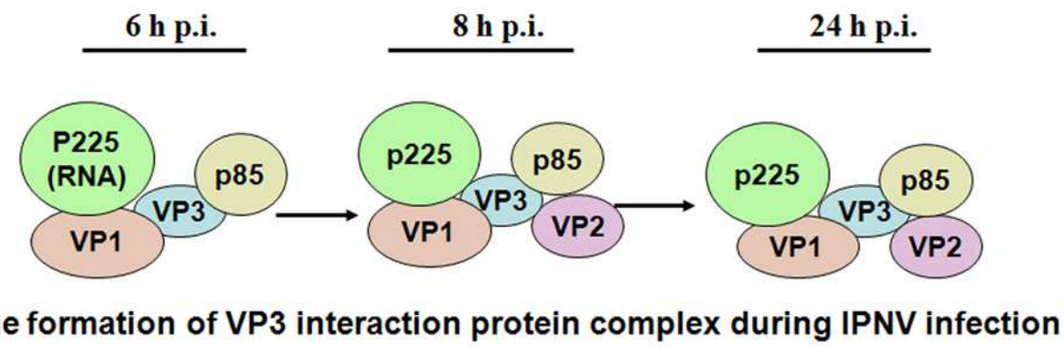

Fig. 5. The interaction between VP3 and other viral components and complexes in IPNV-infected CHSE-214 cells during the replication cycle.
Schematic representation of the IPNV VP3 protein interactions. Early in the replicative cycle (at 6 h p.i.), VP3 interacted with VP1-p85-RNA complex. Then, VP1-p85-RNA-VP3 recruited VP2 at 8 h and 24 h p.i., which may affect either viral replication or viral assembly during the mid to late replication period.

3.5 The role of VP3 protein in cell death

The Bcl-2 family of proteins, including both anti- and pro-apoptotic molecules, act at a critical, intracellular decision point along the common death pathway (Newton and Strasser, 1998). The ratio of antagonist (Bcl-2, Bcl-x_L, Mcl-1, Bcl-W, and A1) to agonist (Bax, Bak, Bcl-x_s, Bid, Bik, Bad, PUMA, and NOXA) molecules dictates whether a cell responds to a proximal apoptotic stimulus (Newton and Strasser, 1998; Galluzzi et al., 2008). Homologues of Bcl-2 (Bcl-xL, Bcl-W, Mcl-1, and A1) reside in mitochondria and stabilize the barrier function of mitochondrial membranes. In contrast, pro-apoptotic proteins can shuttle between non-mitochondrial locations (the cytosol for Bax, Bad, and Bid) and mitochondrial membranes where they can insert and permeabilize the mitochondrial membrane (Zamzami and Kroemer, 2001; Galluzzi et al., 2008). In our system, the Bcl-2 family member, zebrafish Bcl-xL, was found to play a role in blocking both apoptotic (Yang et al., 1995) and necrotic cell death. Recently, VP3 overexpression was found to up-regulate Bad protein (a pro-apoptotic Bcl-2 family member), but how VP3 overexpression was induced remained unknown. Moreover, the interactions of the death domain (80–158 aa) of VP3 protein with other molecules also remained unknown. From the recently published literature, we found that VP3 protein contains a potential phosphokinase C phosphorylation site in Domain 2 corresponding to residues 122–124 (Domain A2; TGR) (Chiu et al., 2010), which could have an important role in cell death induction.

3.6 Novel role for VP3 in the replication cycle

Viruses infect specific target cells, replicate in them to produce large numbers of progeny virions, which then spread to other susceptible cells to initiate new rounds of infection. They also encode proteins that are highly efficient for the optimization of such replication.

However, target organisms use both systemic and cell-based defence mechanisms to limit the extent of viral infection, including immune and inflammatory processes and the execution or suicide of infected cells (Benedict et al., 2002). When we investigated the involvement of viral protein (VP3) in host cell death later in the viral replication cycle (VP3, apoptosis), we found that VP3 interacts with VP1, p85, and RNA initially (Fig. 4, lane 24; Fig. 5), then the VP1-p85-RNA-VP3 complex recruits VP2 at 8 h (Fig. 4, lane 25; Fig. 5) and 24 h (Fig. 4, lane 26; Fig. 5), suggesting that VP3 protein performs many functions. For example, VP3 may stimulate VP1 expression and prime viral assembly. In the present study, VP2 interacted with VP3 protein and a new protein p85 (which may have a role in viral replication), but the role of p85 remains to be elucidated.

4. Conclusion

IPNV E1-S is a fish pathogen of the IPNV Ab strain. It induces apoptotic cell death in CHSE-214 cells (Hong et al., 1998; Hong et al., 1999a; Hong et al., 1999b) and zebrafish ZLE cells (Hong et al., 2005). In summary, we provided evidence that IPNV minor capsid proteins were specifically involved in the induction of necrotic cell death. The death domain of VP3 was found to be located within the stretch 80–158 aa, which contains a protein kinase C phosphorylation site. We also found that the VP3 protein can interact with VP1-p85-RNA complex early in the replicative cycle (at 6 h p.i.), and that VP3-VP1-p85-RNA binds VP2 at 8 h and 24 h p.i. thereby affecting either viral replication or viral assembly. Our study adds important new information concerning the IPNV VP3-host cell interaction and provides the basis for study of the viral pathogenesis of VP3-mediated necrotic cell death and viral assembly.

5. Summary

Aquatic birnavirus induces secondary necrotic cell death through the synthesis of new protein. Very recently we found that the viral genome-encoded minor capsid protein VP3 can induce cell death in fish and mouse cells. In the present study, we identified the death domain of VP3 and the role of VP3 in processes such as interaction with VP1 and viral assembly during late stages of replication. Aquatic birnavirus-encoded *VP3* was mildly expressed in CHSE-214 cells at 4 h post-infection (p.i.), but its expression increased up to 3.5- to 4-fold by 6 h p.i. Furthermore, using a deletion series, the *VP3* death domain was localized to a 78-amino acid (aa) segment (80–158 aa), which was separated from the VP3 self-binding domain (1–101 aa) and VP1 binding domain (the so-called RNA-dependent RNA polymerase, RdRp binding domain; 171–236 aa). Using two anti-VP3 monoclonal antibodies, VP3 was also found to interact with VP1, VP2, viral RNA, and host protein-85. Our results suggested that aquatic birnavirus VP3 not only triggers Bad-mediated cell death, but also stabilizes viral RNA, and promotes viral particle assembly. Thus, VP3 may be a good target for antiviral drug-therapy.

6. Acknowledgments

This work was supported by grants from the National Science Council, Taiwan, Republic of China awarded to Dr. Jainn-Ruey Hong (NSC 96-2313-B-004-MY3 and NSC 99-2321-B-006-010-MY3).

7. References

Benedict, C. A., Norris P. S. and Ware C. F. (2002) To kill or be killed: viral evasion of apoptosis. Nature Immunol. 3:1013-1018.

Chalfie, M., Tu Y., Euskirchen G., Ward W. W. and Prasher D. C. (1994) Green fluorescent protein as a marker for gene expression. Science 263:802-805.

Chen P. C., Wu J. L., Her G. M. and Hong J. R. (2009) Aquatic birnavirus induces necrotic cell death via mitochondria-mediated caspases pathway that inhibited by bongkrekic acid. Fish Shellfish Immunol. 28:344-353.

Chiu C. L., Wu J. L., Her G. M., Chou Y. L. and Hong J. R. (2010) Aquatic birnavirus capsid protein, VP3, induces apoptosis via the Bad-mediated mitochondria pathway in fish and mouse cells. Apoptosis 15(6):653-668.

Dobos, P. (1977). Virus-specific protein synthesis in cells infected by infectious pancreatic necrosis virus. J. Virol. 21:242-258.

Dobos, P., Hill B. J., Hallett R., Kells D. T. C., Becht H. and Tenings D. (1979) Biophysical and biochemical characterization of five animal viruses with bisemented double-stranded RNA genomes. J. Virol. 32:593-605.

Dobos, P. (1995) The molecular biology of infectious pancreatic necrosis virus (IPNV). Annu. Rev. Fish Dis. 5:25-54.

Espinoza, J. C., Hjalmarsson A., Everitt E. and Kuznar J. (2000) Temporal and subcellular localization of infectious pancreatic necrosis virus structural proteins. Arch. Virol. 145:739-748.

Galluzzi L., Brenner C., Morselli E., Touat Z. & Kroemer G. (2008) Viral control of mitochondria apoptosis. PLoS Path 4:1-15.

Hill, B. J. and Way, K. (1995) Serological classification of infectious pancreatic necrosis (IPN) virus and other aquatic birnaviruses. Annu. Rev. Fish Dis. 5:55-77.

Hong, J. R., Lin T. L., Hsu Y. L. and Wu J. L. (1998) Apoptosis precedes necrosis of fish cell line with infectious pancreatic necrosis virus infection. Virology 250:76-84.

Hong, J. R., Hsu Y. L. and Wu J. L. (1999a) Infectious pancreatic necrosis virus induces apoptosis due to down-regulation of survival factor MCL-1 protein expression in a fish cell Virus Res. 63:75-83.

Hong, J. R., Lin T. L., Yang J. Y., Hsu Y. L. and Wu J. L. (1999b) Dynamics of nontypical apoptotic morphological changes visualized by green fluorescent protein in living cells with infectious pancreatic necrosis virus infection. J. Virol. 73:5056-5063.

Hong, J. R. and Wu J. L. (2002a) Molecular regulation of cellular apoptosis by fish infectious pancreatic necrosis virus (IPNV) infection. Curr. Top. Virol. 2:151-160.

Hong, J. R. and Wu J. L. (2002b) Induction of apoptotic death in cells via bad gene expression by infectious pancreatic necrosis virus infection. Cell Death Differ. 9:113-124.

Hong, J. R., Gong H. Y. and Wu J. L. 2002c. IPNV VP5, a novel anti-apoptosis gene of the Bcl-2 family, regulates Mcl-1 and viral protein expression. Virology 295:217-229.

Hong, J. R., Huang L. J. andWu J. L. (2005) Aquatic birnavirus induces apoptosis through activated caspase-8 and -3 in a zebrafish cell line. J. Fish Dis. 28:133-140.

Hong, J. R., Guan B. J., Her G. M., Evensen O., Santi N. and Wu L. L. (2008) Aquatic birnavirus infectious activates the transcription factor NF-kB via tyrosine kinase signaling leading to cell death. J. Fish Dis. 31:451-460.

Hudson P. J, McKern N. M, Power B. E, and Azad A. A. (1986) Genomic structure of the large RNA segment of infectious bursal disease virus. Nucleic Acids Res. 14:5001-5012.

Hwang H. J., Moon C. H., Kim J. Y., Lee J. M., Park J. W. and Chung D. K. (2007) Identification and functional analysis of salmon annexin 1 induced by a virus infection in a fish cell line. J. Virol. 81:13816-24.

Kain, S. R., Mai K. and Sinai P. (1994) Human multiple tissue Western blots: a new immunological tool for the analysis of tissue-specific protein expression. BioTechniques 17:982-987.

Laemmli, U. K. (1970) Cleavage of structural proteins during the assembly of the head of bacteriophage T4. Nature 227:680-685.

Maniak, M., Rauchenberger R., Albrecht R., Murphy J. and Gerisch G. (1995) Coronin involved in phagocytosis: dynamics of particle-induced relocalization visualized by a green fluorescent protein tag. Cell 83:915-924.

Newton, K. and Strasser A. (1998) The Bcl-2 family and cell death regulation. Curr. Opin. Genet. Dev. 8:68-75.

Nicholson, B. and Dunn J. (1974) Homologous viral interference in trout and Atlantic salmon cell cultures infected with infectious pancreatic necrosis. J. Virol. 14:180-182.

Oparka, K. J., Roberts A. G., Santa-Cruz S., Boevink P., M. Prior D. A. and Smallcobe A. (1997) Using GFP to study virus invasion and spread in plant tissues. Nature 388:401-402.

Pedersen T., Skjesol A. and Jorgensen J. A. (2007) VP3, a structural protein of infectious pancreatic necrosis virus, interacts with RNA-dependent polymerase VP1 and with double-stranded RNA. J Virol. 81:6652-6663.

Studier F. W. (1973) Analysis of bacteriophage T7 early RNA's and proteins in slab gels. Journal of Molecular Biology 79:237-248

Wang W. L., Hong J. R., Lin G. H., Liu W. T., Gong H. Y., Lu M. W., Lin C. C. and Wu J. L. (2011) Stage-Specific Expression of TNFα Regulates Bad/Bid-Mediated Apoptosis and RIP1/ROS-Mediated Secondary Necrosis in Birnavirus-Infected Fish Cells. PloS ONE 6: e16740.

Wu, J. L., Chang C. Y. and Hsu Y. L. (1987) Characteristics of an infectious pancreatic necrosis like virus isolated from Japanese eel (*Anguilla japonina*). Bull. Inst. Zool. Acad. Sinica 26:201-214.

Wu, J. L., Hong J. R., Chang C. Y., Hui C. F., Liao C. F. and Hsu Y. L. (1998) Involvement of serine proteinase in infectious pancreatic necrosis virus capsid protein maturation and NS proteinase cleavage in CHSE-214 cells. J. Fish Dis. 21:215-220.

Villanueva R. A, Galaz J. L, Valdes J. A, Jashes M. M. and Sandina A. M. (2004) Genome assembly and maturation of the birnavirus infectious pancreatic necrosis virus. J. Virol. 78:13829-13838.

Yang, E., Zha J., Jokel J., Boise L. H., Thompson C. B. and Korsmeyer S. J. (1995) Bad, a heterodimeric partner for Bcl-XL and Bcl-2, displaces Bax and promotes cell death. Cell 80:285-291.

Zamzami, N. and Kroemer G. (2001) The mitochondria in apoptosis: how Pandora's box opens. Nat. Rev. Mol. Cell Biol. 2:67-71.

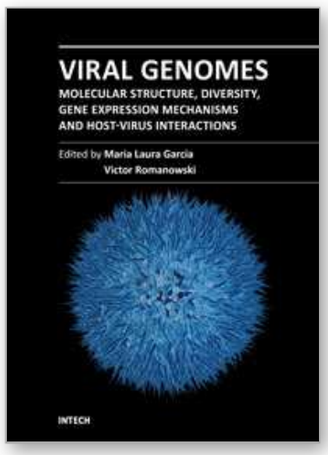

Viral Genomes - Molecular Structure, Diversity, Gene Expression Mechanisms and Host-Virus Interactions

Edited by Prof. Maria Garcia

ISBN 978-953-51-0098-0
Hard cover, 302 pages
Publisher InTech
Published online 24, February, 2012
Published in print edition February, 2012

Viruses are small infectious agents that can replicate only inside the living cells of susceptible organisms. The understanding of the molecular events underlying the infectious process has been of central interest to improve strategies aimed at combating viral diseases of medical, veterinary and agricultural importance. Some of the viruses cause dreadful diseases, while others are also of interest as tools for gene transduction and expression and in non-poluting insect pest management strategies. The contributions in this book provide the reader with a perspective on the wide spectrum of virus-host systems. They are organized in sections based on the major topics covered: viral genomes organization, regulation of replication and gene expression, genome diversity and evolution, virus-host interactions, including clinically relevant features. The chapters also cover a wide range of technical approaches, including high throughput methods to assess genome variation or stability. This book should appeal to all those interested in fundamental and applied aspects of virology.

INTECH
open science | open minds

InTech Europe
University Campus STeP Ri
Slavka Krautzeka 83/A
51000 Rijeka, Croatia
Phone: +385 (51) 770 447
Fax: +385 (51) 686 166
www.intechopen.com

InTech China
Unit 405, Office Block, Hotel Equatorial Shanghai
No.65, Yan An Road (West), Shanghai, 200040, China
中国上海市延安西路65号上海国际贵都大饭店办公楼405单元
Phone: +86-21-62489820
Fax: +86-21-62489821

IntechOpen